



1 **Harmonized chronologies of a global late Quaternary pollen**
2 **dataset (LegacyAge 1.0)**

3 Chenzhi Li^{1,2}, Alexander K. Postl¹, Thomas Böhmer¹, Xianyong Cao³, Andrew M. Dolman¹,
4 Ulrike Herzschuh^{1,2,4}

5 ¹ Alfred Wegener Institute, Helmholtz Centre for Polar and Marine Research, Polar Terrestrial Environmental
6 Systems, Telegrafenberg A45, 14473 Potsdam, Germany

7 ² Institute of Environmental Science and Geography, University of Potsdam, Karl-Liebknecht-Str. 24-25, 14476
8 Potsdam, Germany

9 ³ Alpine Paleocology and Human Adaptation Group (ALPHA), State Key Laboratory of Tibetan Plateau Earth
10 System, and Resources and Environment (TPESRE), Institute of Tibetan Plateau Research, Chinese Academy of
11 Sciences, 100101 Beijing, China

12 ⁴ Institute of Biochemistry and Biology, University of Potsdam, Karl-Liebknecht-Str. 24-25, 14476 Potsdam,
13 Germany

14 **Correspondence:** Ulrike Herzschuh (Ulrike.Herzschuh@awi.de)

15 **Abstract.** Although numerous pollen records are available worldwide in various databases, their use for synthesis
16 works is limited as the chronologies are, as yet, not harmonized globally, and temporal uncertainties are unknown.
17 We present a chronology framework named LegacyAge 1.0 that includes harmonized chronologies of 2831
18 palynological records (out of 3471 available records), downloaded from the Neotoma Paleocology Database (last
19 access: April 2021) and 324 additional Asian records. All chronologies use the Bayesian framework implemented
20 in Bacon version 2.5.3. Optimal parameter settings of priors (accumulation.shape, memory.strength,
21 memory.mean, accumulation.rate, thickness) were identified based on previous experiences or iteratively after
22 preliminary model inspection. The most common control points for the chronologies are radiocarbon dates
23 (86.1%), calibrated by the latest calibration curves (IntCal20 and SHcal20 for the terrestrial radiocarbon dates in
24 the northern and southern hemispheres; Marine20 for marine materials). The original literature was consulted
25 when dealing with obvious outliers and inconsistencies. Several major challenges when setting up the



26 chronologies included the waterline issue (18.8% of records), reservoir effect (4.9%), and sediment deposition
27 discontinuity (4.4%). Finally, we numerically compare the LegacyAge 1.0 chronologies to the original ones and
28 show that the chronologies of 95.4% of records could be improved according to our assessment. Our chronology
29 framework and revised chronologies provide the opportunity to make use of the ages and age uncertainties in
30 synthesis studies of, for example, pollen-based vegetation and climate change. The LegacyAge 1.0 dataset and R
31 code used are open-access and available at PANGAEA (<https://doi.pangaea.de/10.1594/PANGAEA.933132>; Li
32 et al., 2021) and Github (<https://github.com/LongtermEcology/LegacyAge-1.0>), respectively.

33 **1 Introduction**

34 Global and continental fossil pollen databases are used for a variety of paleoenvironmental studies, such as past
35 climate and biome reconstructions, palaeo-model validation, and the assessment of human-environmental
36 interactions (Gajewski, 2008; Gaillard et al., 2010; Cao et al., 2013; Mauri et al., 2015; Trondman et al., 2015;
37 Marsicek et al., 2018; Herzschuh et al., 2019). Several fossil pollen databases have been successfully established
38 (Gajewski, 2008; Fyfe et al., 2009), such as the European Pollen Database
39 (<http://www.europeanpollendatabase.net>), the North American Pollen Database
40 (<http://www.ncdc.noaa.gov/paleo/napd.html>), and the Latin American Pollen Database
41 (<http://www.latinamericapollendb.com>); most of these data are now included in the Neotoma Paleocology
42 Database (<https://www.neotomadb.org/>; Williams et al., 2018). Chronologies and control points are stored in these
43 databases along with the pollen records. However, the inference of temporal uncertainty remains a challenge
44 because they are based on calibrated and uncalibrated ¹⁴C ages and were established using various methodologies
45 (Blois et al., 2011; Giesecke et al., 2014; Flantua et al., 2016; Trachsel and Telford, 2017). Recently, the need for
46 harmonized chronologies and an identical inference of temporal uncertainties have increased as studies are looking
47 for spatiotemporal patterns using multi-record analyses (Jennerjahn et al., 2004; Blaauw et al., 2007; Giesecke et
48 al., 2011; Flantua et al., 2016). Accordingly, some efforts have been made to harmonize the chronologies for part
49 of the data stored in the databases (Fyfe et al., 2009; Blois et al., 2011; Giesecke et al., 2011; Giesecke et al., 2014;
50 Flantua et al., 2016; Brewer et al., 2017; Wang et al., 2019; Mottl et al., 2021). However, a harmonized
51 chronology framework is needed, not only to allow for the consistent inference of age and age uncertainties but
52 also to apply to newly published records or one that can be adjusted to the specific requirement of a study.



53 Here we present the rationale and code for the chronology framework named LegacyAge 1.0, as well as the
54 metadata, and parameter settings of 2831 palynological records from the Neotoma Paleocology Database (last
55 access: April 2021) and 324 additional Asian records that were recently synthesized (Cao et al., 2013, 2020). We
56 also report on the major challenges when setting up the chronologies and assess the quality of the LegacyAge 1.0
57 chronologies. Finally, the newly harmonized chronologies are numerically compared with the original ones. All
58 data and R code used for this study are open-access and available at PANGAEA
59 (<https://doi.pangaea.de/10.1594/PANGAEA.933132>; Li et al., 2021) and Github
60 (<https://github.com/LongtermEcology/LegacyAge-1.0>), respectively.

61 2 Methods

62 2.1 Data sources

63 We established chronologies for the ‘Global taxonomically harmonized pollen data collection with revised
64 chronologies’ (<https://doi.pangaea.de/10.1594/PANGAEA.929773>; Herzschuh et al., 2021), which comprises
65 3471 records (3147 records from Neotoma (last access: April 2021) and 324 records from Asian datasets). Records
66 were obtained from lake sediments (49.4%), peatlands (34.3%), and other archives (16.3%) (Fig. 1). As the spatial
67 coverage of records in certain regions is poor, for example, in China and Siberia, records compiled by Cao et al.
68 (2013, 2020) and our own collection (AWI) were included. The following chronology metadata were collected
69 for each record: *Event*, *Data_Source*, *Site_ID*, *Dataset_ID*, *Site_name*, *Location* (*longitude*, *latitude*, *elevation*,
70 *and continent*), *Archive_Type*, *Site_Description*, *Reference*, *Laboratory number of dating*, *Dating_Method*,
71 *Material_Dated*, *Date* (*age*, *error older*, *error younger*, *depth*, *thickness*), *Additional relevant comments from*
72 *authors* (*e.g., reservoir effect, hiatus, outliers, and date rejected*), *Original chronologies* (*name*, *age type*
73 (*calibrated or uncalibrated radiocarbon years BP*), *age model*, *estimated age* (*age older*, *age*, *age younger*),
74 *control points* (*e.g., core top, core bottom, and control point type*)). This dataset is available at
75 <https://doi.pangaea.de/10.1594/PANGAEA.933132> (Li et al., 2021).

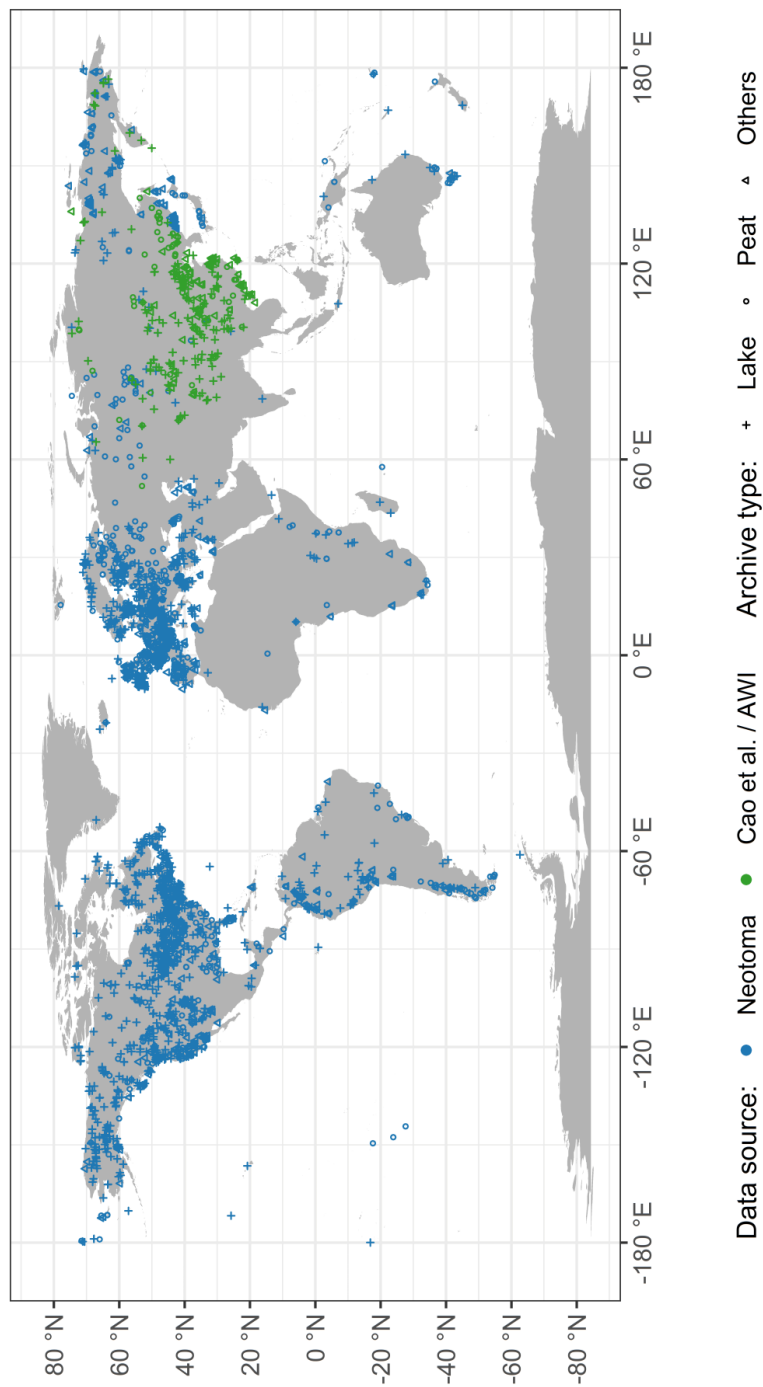


Figure 1. Map of records by source and archive type.



77 **2.2 Chronological control points**

78 **2.2.1 Radiometric dates**

79 **Radiocarbon dating:** most records are dated by radiocarbon method (^{14}C dating, conventional or accelerator mass
80 spectrometry), which is one of the most commonly used dating techniques as it covers the time range of most
81 pollen records (ca. the last 50 ka BP (before present)). However, ^{14}C dates can appear to be too old or too young
82 due to various effects such as the reservoir effect, contamination, and insufficient carbon, which have to be
83 considered when setting up the chronologies (Roberts, 2013).

84 **Lead-210 dating:** the uppermost part of some lake records have been dated using a radioactive isotope of lead
85 (lead-210), which has a half-life of 22.3 years and provides useful age control for the last 100-150 years (Appleby
86 and Oldfield, 1978; Cuney, 2021).

87 **Luminescence dating:** archaeological materials, loess, and river sediments have often been dated via
88 luminescence, including thermoluminescence (TL) and optically stimulated luminescence (OSL). These dating
89 techniques cover time-scales from millennia to hundreds of thousands of years (Roberts, 2013; Cuney, 2021).

90 **2.2.2 Lithological dates**

91 **Varve dating:** varve chronology, generated from counting varves, is considered a relatively accurate dating
92 method for the late Quaternary, particularly for the Holocene (Ojala et al., 2012; Zolitschka et al., 2015; Ramisch
93 et al., 2020). All samples are considered as control points. If a pollen record has a varve chronology stored and
94 assessed in the Varved Sediments Database (VARDA, <https://varve.gfz-potsdam.de/>), we generally preferred to
95 use it over chronologies based on other dating techniques.

96 **Tephrochronology:** tephra layers are used as isochrones to correlate and synchronize sequences at a regional or
97 continental scale (Lowe, 2011). Tephrae documented in the Global Tephrochronological Database (Tephabase,
98 <https://www.tephrbase.org/>) were included to improve the chronologies (in accordance with Giesecke et al.,
99 2014), such as the Mazama ash (7630 \pm 40 cal. yr BP (where ‘present’ is 1950 CE); Brown and Hebda, 2003),
100 Vedde ash (12121 \pm 57 cal. yr BP; Lane et al., 2012), and the Laacher See ash (12880 \pm 120 cal. yr BP).

101 **2.2.3 Biostratigraphical dates**



102 Biostratigraphical dates have been widely relied on before ^{14}C dating became available and affordable (Bardossy
103 and Fodor, 2013). Since the biostratigraphic schemes are updated by new records, improved dating, and taxonomic
104 revision (Flantua et al., 2016), most of them were rejected when we harmonized the chronologies. However, a
105 few well-known and widely applicable biostratigraphic boundaries (Rasmussen et al., 2014) were used if the
106 chronologies could not be sufficiently constrained by other dating techniques, for example, the Younger
107 Dryas/Holocene (11500 ± 250 cal. yr BP), Allerød/Younger Dryas (12650 ± 250 cal. yr BP), and Oldest
108 Dryas/Bølling (14650 ± 250 cal. yr BP; Giesecke et al., 2014).

109 **2.3 Establishing the chronologies**

110 **2.3.1 Method choice**

111 Establishing age-depth relationships is necessary because sediment cores typically have fewer chronological
112 control points than samples and to account for dating uncertainty. A number of methods are available including
113 linear interpolation, smoothing spline, OxCal, Bchron, and Bacon (Bennett and Fuller, 2002; Blaauw, 2010;
114 Blaauw and Heegaard, 2012; Flantua et al., 2016; Sánchez Goñi et al., 2017; Trachsel and Telford, 2017; Blaauw
115 et al., 2018). Bacon is one of the most commonly used methods for age-depth modeling that ‘uses Bayesian
116 statistics to reconstruct Bayesian accumulation histories for deposits, through combining radiocarbon and other
117 dates with prior information’ (Blaauw and Christen, 2011). The collection of additional information, on the
118 geological and hydrological setting as well as the environmental history (Giesecke et al., 2014), helps to constrain
119 the chronologies, although it is time-consuming for large datasets. Through millions of Markov Chain Monte
120 Carlo (MCMC) iterations, Bacon provides the calibrated ages (mean, median, minimum, maximum) at each depth
121 (e.g., every centimeter) with a 95% confidence intervals and an indication of how well the model fits the dates,
122 although it needs much supervision and computing power. The confidence interval guides the overall trend of the
123 age-depth relationships, so the control points guide rather than strictly constrain the age-depth relationships
124 (Giesecke et al., 2014). Bacon version 2.3.3 and later (Blaauw and Christen, 2011) can also handle sudden shifts
125 in the accumulation rate when given the hiatus/boundary depth and resetting the memory to 0 when crossing the
126 hiatus. Therefore, all age-depth relationships in our dataset will be constructed using the latest Bacon version 2.5.3
127 (Blaauw and Christen, 2011; Blaauw et al., 2018) in R (R Core Team, 2021).

128 **2.3.2 Core tops and basal ages**



129 Wherever possible, the record-related publications were read to decide whether the core top was modern at the
130 time of sampling. For modern core-tops, if the core was collected from sites where sediment was still accumulating,
131 the sediment surface could be assigned to the year of sampling, adding one significant time control for the
132 chronologies. If the sampling date was unavailable, an alternative surface age from the original chronology in
133 Neotoma was added at the core top. For core-tops judged not to be modern, we inferred the surface age from the
134 calibrated age-depth model. For basal ages, when the calibrated age-depth model for the lowermost profile has
135 considerable extrapolation and was not sufficiently constrained by the control points, we also accepted the prior
136 information of core basal age from the record-related publications or Neotoma. Moreover, the highest (lowest)
137 depth of the model was defined by the first (last) dating or pollen sample.

138 2.3.3 Calibration curves

139 To transform the measured ^{14}C ages to calendar ages, the latest calibration curves were used (Hajdas, 2014):
140 IntCal20 (Reimer et al., 2020) and SHcal20 (Hogg et al., 2020) to calibrate the terrestrial radiocarbon dates in the
141 northern and southern hemispheres, respectively; and Marine20 (Heaton et al., 2020) for the 38 marine records
142 included in our dataset although it does not distinguish between the northern and southern hemisphere (Sánchez
143 Goñi et al., 2017). Absolute dates (e.g., lead-210, OSL, tephra), already presented on the calendar scale, were not
144 calibrated (Blaauw and Christen, 2011). Modern/post-bomb ^{14}C dates (negative ^{14}C ages) were calibrated using
145 appropriate post-bomb calibration curves (post-bomb=1 for $>40^\circ\text{N}$; 2 for $0^\circ\text{-}40^\circ\text{N}$; 4 for southern hemisphere;
146 Hua et al., 2013).

147 2.3.4 Parameter settings for the initial Bacon run

148 After consultation of the relevant literature (Blaauw and Christen, 2011; Goring et al., 2012; Cao et al., 2013;
149 Fiałkiewicz-koziół et al., 2014; Blaauw et al., 2018) and assessments of several runs with a test set of records, we
150 set the following Bacon parameters. (1) The prior for the accumulation rate consists of a gamma distribution with
151 two parameters, **mean accumulation rate** (acc.rate) and **accumulation shape** (acc.shape). For the acc.shape, we
152 accepted its default value of 1.5 as higher values resulted in a more peaked shape of the gamma distribution. A
153 first approximation of the acc.mean was calculated as the average accumulation rate between the first and the last
154 date of each record, combined with the prior information of dates, which is more reasonable than using a constant
155 value (default acc.mean=20 yr/cm). (2) The **section thickness** (default thick=5) significantly affects the flexibility



156 of the age-depth model. Blaauw and Christen (2011) indicated that models with few sections tend to show more
157 abrupt changes in accumulation rate, while models with many sections usually appear smoother but are
158 computationally more intense. We tested six thicknesses (2.5 cm, 5 cm, 10 cm, 30 sections, 60 sections, and 120
159 sections) with and without an artificial surface age, thereby generating 12 age models for each core. (3) The
160 memory, that is, the dependence of accumulation rate between neighboring depths, is a beta distribution defined
161 by two parameters: **memory strength** (mem.strength; default 10) and **mean memory** (mem.mean; default 0.5).
162 For the mem.strength, we used a value of 20 as suggested by Goring et al. (2012), which allows a large range of
163 posterior memory values. We set different mem.mean values (0.3 for lake and 0.7 for peatland) to accommodate
164 differences in accumulation conditions between lakes and peatland, where the higher memory for peatlands
165 implies a more constant accumulation history (Blaauw and Christen, 2011; Goring et al., 2012; Cao et al., 2013;
166 Cao et al., 2020).

167 In addition to the major parameters mentioned above, we also adjusted several specific parameters for some
168 records according to prior information collected from record-related publications or Neotoma (this table is
169 available in PANGAEA). (1) **Freshwater reservoir effects**: the uptake of old carbon by aquatic plants, the ‘hard-
170 water effect’ or slow CO₂ exchange between the atmosphere and water, can result in too old radiocarbon dates
171 (Philippsen, 2013; Philippsen and Heinemeier, 2013). In addition to the reservoir ages reported by the original
172 authors, we also identified some additional records, where the authors may have ignored them via modern
173 correction and linear extrapolation (Wang et al., 2017). We then subtracted the reservoir age from all ¹⁴C dates of
174 an affected record as a constant. We may have underestimated the number of such records due to the difficulty of
175 estimating the reservoir age where the sediment surface was eroded or used for agricultural purposes. (2)
176 **Waterline issues**: stratigraphic records do not always start at a depth of 0 cm, for example, if the uppermost part
177 of the core is lost, if the record is only a part of a longer sequence, or if the depths are measured from the water
178 surface instead of the sediment surface, leading to the so-called waterline issue. Accordingly, we adjusted the
179 uppermost depth of the chronology based on prior information collected from the original publications and
180 Neotoma. (3) **Hiatuses**: where the sediment deposition was not continuous, Bacon resets the memory to 0, causing
181 a break in auto-correlated in the accumulation rate for depths before and after the hiatus (Blaauw and Christen,
182 2011). (4) **Dates rejected/added**: Neotoma usually reports all ¹⁴C dates from cores, even when deemed inaccurate.
183 We assessed and, if appropriate, a priori rejected the ¹⁴C dates of samples with contaminated or insufficient carbon,
184 or reworked sediments, in most cases following the suggestions in the original publications. We down-weighted



185 the impact of outliers on the overall trend of the age-depth relationships and risked that age uncertainties were too
186 optimistic. We also documented all lithological dates (e.g., varves and tephra) and biostratigraphical dates
187 collected from the original publications and from Neotoma to supplement the chronology metadata.

188 **2.3.5 Assessment of initial age-depth models and final parameter selection**

189 For each record, 12 age models were visually assessed. Preference was given to models that fitted the dates well
190 and with small uncertainties when choosing the ‘best’ model for each record (Blaauw and Christen, 2011; Blaauw
191 et al., 2018). If necessary, we also adjusted the parameter settings such as the section thickness and accumulation
192 rate to make a better fit with the dates that was consistent with prior information. For the final parameter settings
193 used for each record, please see <https://doi.pangaea.de/10.1594/PANGAEA.933132> (Li et al., 2021).

194 **2.4 Evaluation of the newly generated age-depth models**

195 For the temporal uncertainty of the age-depth models, we take used the 95% confidence intervals for age estimated
196 by the Bacon model for each centimeter. These values are approximately twice the standard error of the estimated
197 age at a given depth. We plotted our newly generated calibrated chronologies with 95% confidence intervals
198 together with the original ones taken from the Neotoma and Cao et al. (2013, 2020) datasets to make comparisons
199 and evaluate the performance of the new models.

200 **3 Results**

201 **3.1 Overview of major challenges when establishing the chronologies**

202 Age-depth models were initially established for all 3471 records. We discarded 640 records with fewer than 2
203 reliable dates and leaving chronologies for 2831 records. We faced several major challenges when establishing
204 the chronologies. After assessments and consultation of prior information from original publications, we identified
205 139 records (4.9%) with reservoir effects, 533 records (18.8%) with waterline issues, 125 records (4.4%) with
206 hiatuses, 924 records (32.6%) with rejected or added dates, and 743 records (26.2%) that contained several of the
207 above problems: all these challenges have been handled (Fig. 2). After assessing initial age-depth models,
208 accumulation rates were adjusted for 367 records (13.0%), and different section thicknesses were applied to 411
209 records (14.5%).

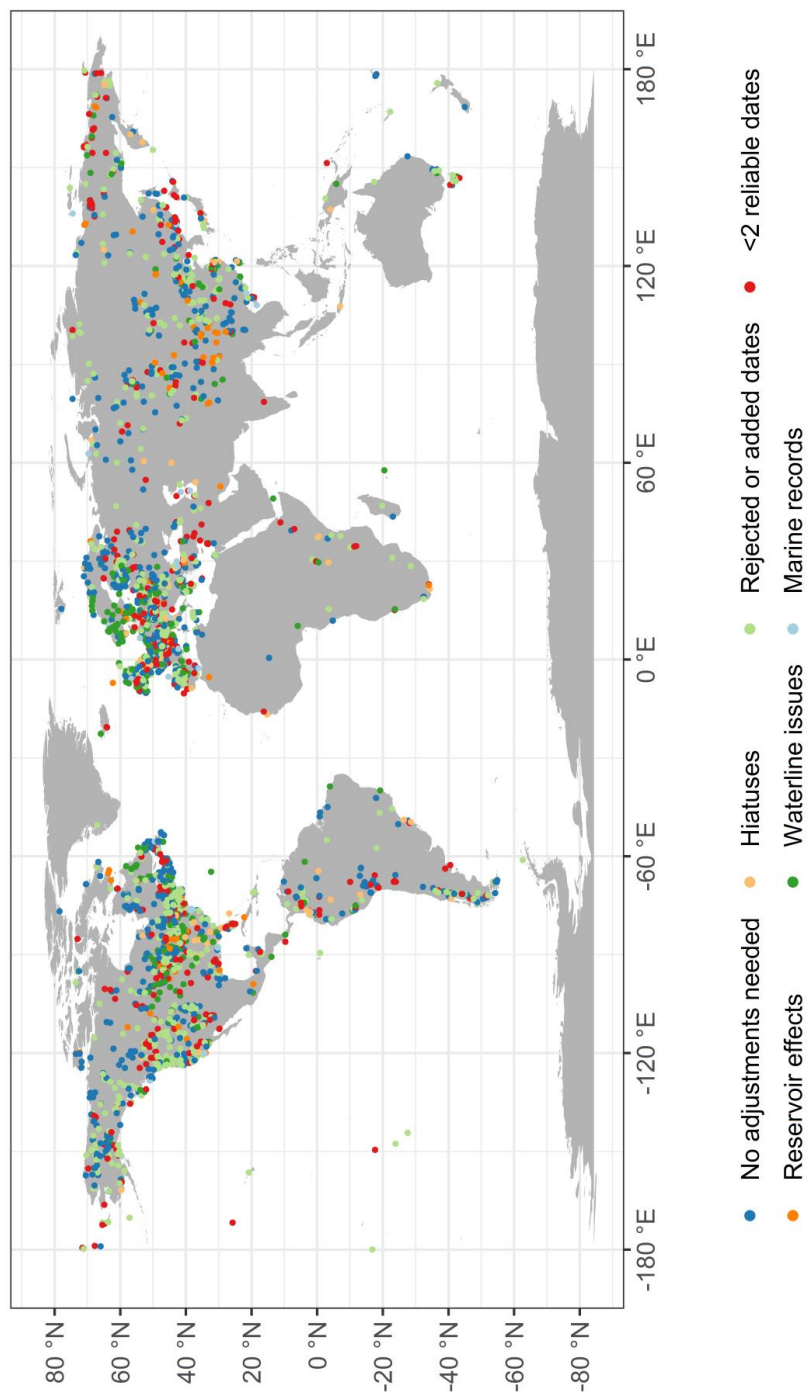


Figure 2. The distribution of records that faced various major challenges when establishing their chronologies.



211 **3.2 LegacyAge 1.0 quality**

212 **3.2.1 Dates used for final chronologies**

213 A total of 19,990 control points (out of 21,199 dates available) were used to generate the chronologies for the
214 2831 records. Among them, the most common chronological control points are radiocarbon dates (86.1%),
215 followed by lithological and biostratigraphical dates (8.5%) collected from publications or Neotoma, and lead-
216 210 (5.0%); other dating techniques make up 0.4% of the control points. The median number of dates per
217 chronology is 5, with 23.3% of the chronologies having 2 or 3 dates, 53.3% having 4-8 dates, and 23.4% having
218 at least 9 dates (Fig. 3).

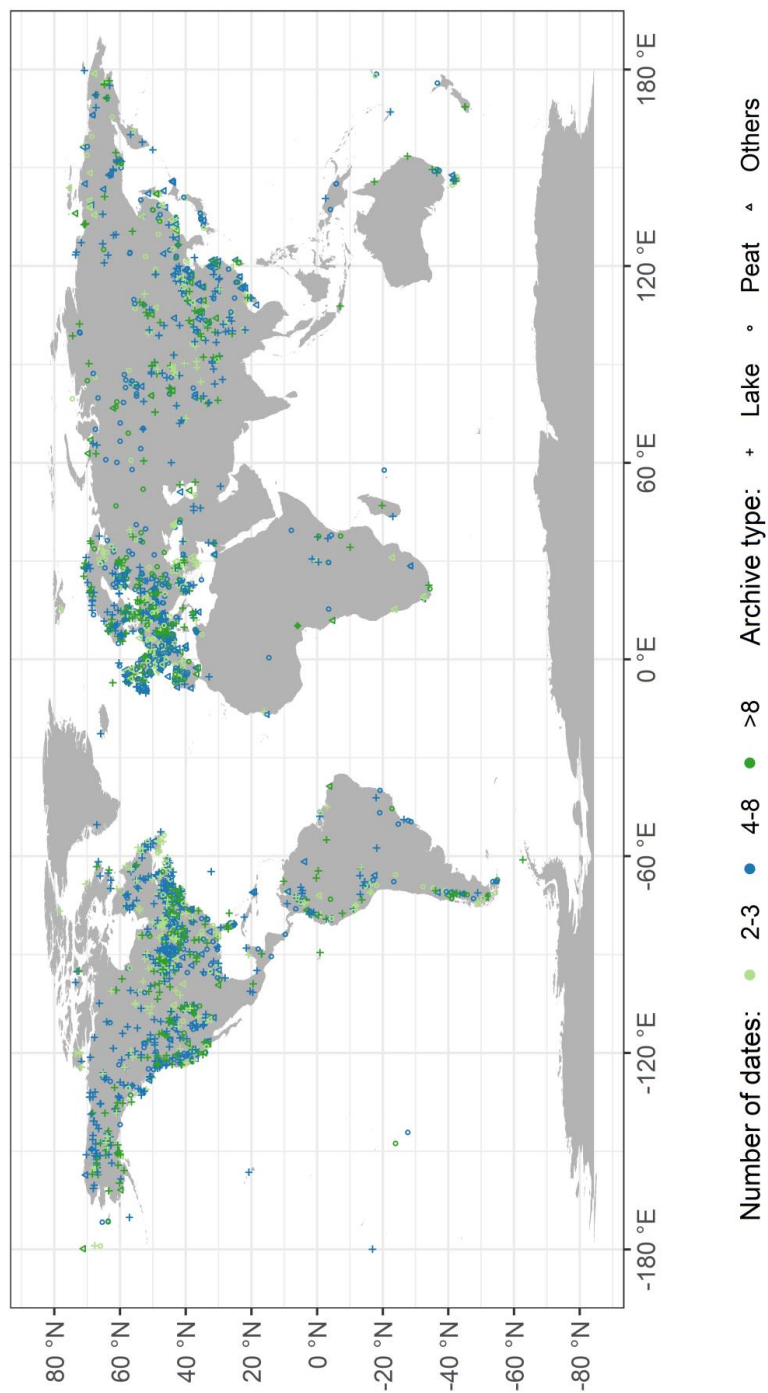
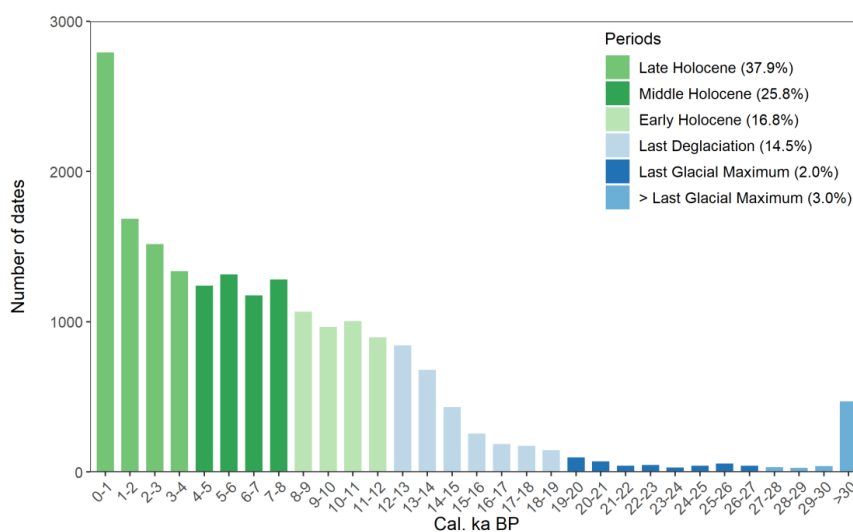


Figure 3. Map of the number of dates and archive types for each record.



220 Currently, 80.5% of chronological control points in the LegacyAge 1.0 fall within the Holocene (37.9%, 25.8%,
221 and 16.8% within the late (ca. 0–4.2 cal. ka BP), middle (ca. 4.2–8.3 cal. ka BP), and early Holocene (ca. 8.3–11.7
222 cal. ka BP), respectively), 14.5% within the Last Deglaciation (ca. 19.0–11.7 cal. ka BP; Clark et al., 2012), 2.0%
223 within the Last Glacial Maximum (ca. 26.5–19.0 cal. ka BP; Clark et al., 2009), and only 3.0% earlier than the
224 LGM (Fig. 4).



225

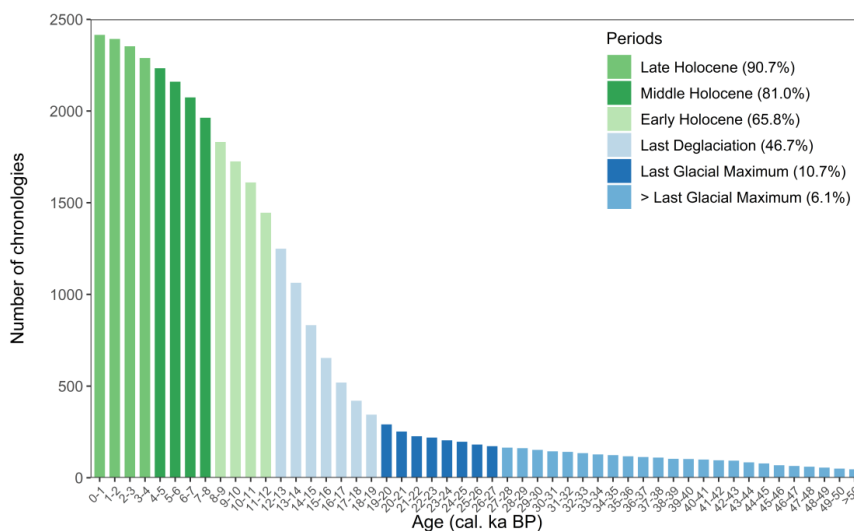
226

Figure 4. Histogram showing the number of available dates in distinct time slices.

227 3.2.2 Spatial and temporal coverage

228 Of the 2831 chronologies finally established, 1032 records are from North America, 1075 records from Europe,
229 488 records from Asia, 150 records from South America, 54 records from Africa, and 32 records from the Indo-
230 Pacific (Fig. 3). Most records (2659 records, 93.9%) are in the northern hemisphere, where the main vegetation
231 and climate zones are covered.

232 As shown in Fig. 5, 94.8% of chronologies cover part of the last 30 ka, while Marine Isotope Stage 3 (MIS-3)
233 is relatively poorly covered. Specifically, 98.0% of chronologies cover part of the Holocene (90.7%, 81.0%, and
234 65.8% cover part of the late, middle, and early Holocene, respectively), 46.7% cover part of the Last Deglaciation,
235 10.7% cover part of the Last Glacial Maximum, and only 6.1% earlier than LGM.



236

237

Figure 5. Histogram showing the number of available chronologies in distinct time slices.

238

3.2.3 Temporal uncertainty

239

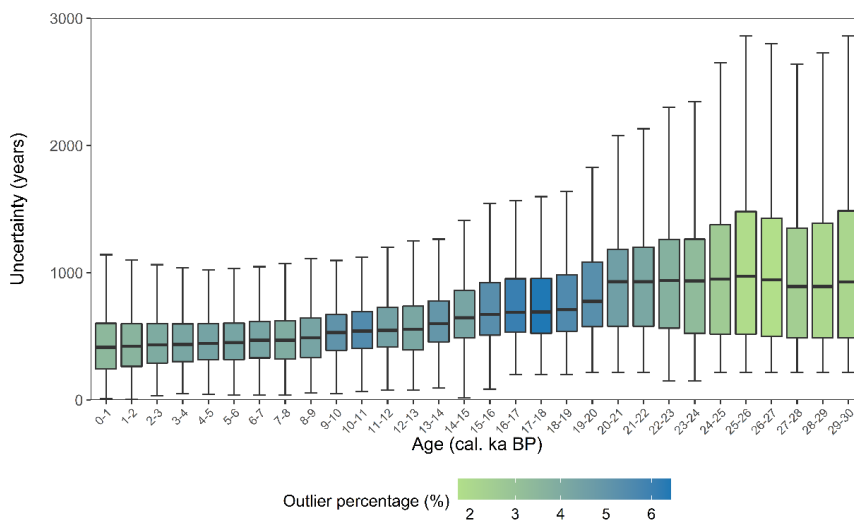
Boxplots of age uncertainties for all chronologies in distinct time slices, excluding outliers (ca. 4.2%), illustrate

240

that age uncertainty tends to increase with age and are mainly related to the uncertainties of the chronological

241

control points and the uncertainty of the calibration curves (Fig. 6).



242



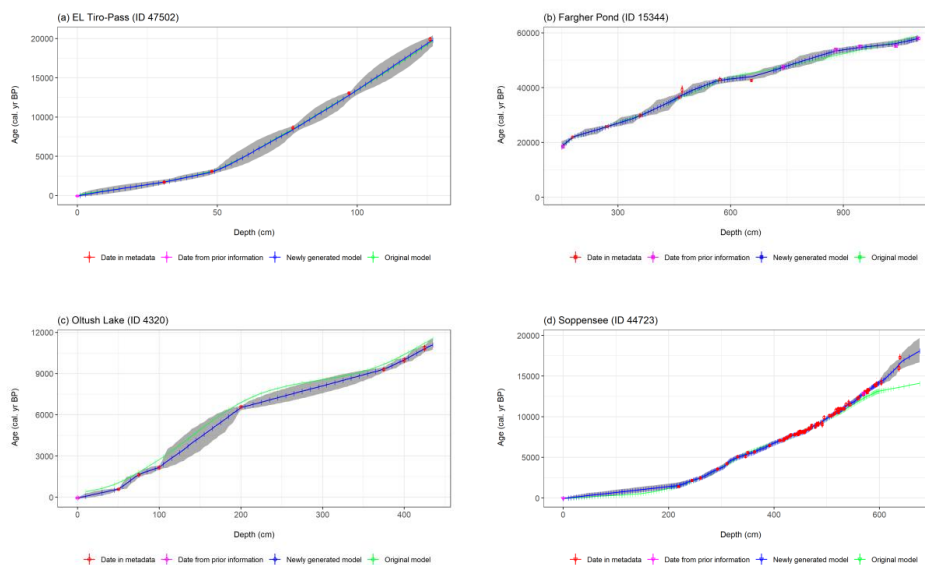
243 **Figure 6.** Boxplots of age uncertainties and outlier percentages in distinct time slices.

244 3.3 Comparison of the LegacyAge 1.0 vs. original age-depth models

245 For 906 records out of the 2831 records included in the LegacyAge 1.0, no calibrated chronologies were originally
246 available from the Neotoma and Cao et al. (2013, 2020) datasets for comparison. Of the remaining 1925 records,
247 the new LegacyAge 1.0 chronologies were selected instead of the original ones in 95.4% of cases. Where original
248 chronologies outperformed LegacyAge 1.0, it is mainly because they are varve chronologies, had incomplete
249 metadata (e.g., missing sample depths), or they included some non-¹⁴C dates that our model could not
250 accommodate.

251 In most cases, the newly established chronologies were rather similar to the original ones. For 1012 records
252 (52.6% of 1925 records), the original chronologies were within the 95% confidence intervals of the LegacyAge
253 1.0 chronologies, while the other 913 records (47.4%) were partially or completely outside the 95% confidence
254 intervals.

255 Selected typical examples of the comparison results between the newly generated and original chronologies are
256 illustrated in Fig. 7. For the *EL Tiro-Pass* record (ID 47502, Fig. 7a), both the original and newly generated
257 chronologies were established by Bacon and are acceptable. However, our newly generated chronology has the
258 advantage that it makes use of the latest radiocarbon calibration curve (IntCal20; Reimer et al., 2020), and the
259 estimated surface age is more realistic as sediments are still accumulating (Niemann and Behling, 2008). For the
260 *Fargher Pond* record (ID 15344, Fig. 7b), our newly generated chronology includes more varve ages from the
261 Varved Sediments Database. These provide a better constraint for the lowermost profile than the original model
262 had (Grigg and Whitlock, 2002). For the *Oltush Lake* record (ID 4320, Fig. 7c), the ¹⁴C age of modern sediment
263 in this lake is 350 yr BP and thus the assumption of a reservoir effect of 350 years resulted in slightly younger
264 ages than originally given (Davydova and Servant-Vildary, 1996). Finally, for the *Soppensee* record (ID 44723,
265 Fig. 7d), most of the ¹⁴C dates (> 540 cm) have insufficient carbon (Hajdas and Micezyński, 2010) and thus the
266 original chronology, generated from counting varves, outperformed our newly generated chronology.



267

Figure 7. Comparison of newly generated age-depth models with the original ones.

268 4 Code and data availability

269 All data and R code used for this study are available at PANGAEA
270 (<https://doi.pangaea.de/10.1594/PANGAEA.933132>; Li et al., 2021) and Github
271 (<https://github.com/LongtermEcology/ProxyAge-1.0>), respectively.

272 5 Conclusion

273 This paper presents the framework as well as metadata, R pipeline, chronologies, and age uncertainties of 2831
274 pollen palynological records synthesized from the Neotoma Paleocology Database (last access: April 2021) and
275 324 additional Asian records (Cao et al., 2013, 2020). Chronologies and uncertainties can be used from synthesis
276 works; metadata and pipeline can be used to reestablish the chronologies for customized purposes, and the
277 framework can be used for establishing chronologies for new records.

278 **Author contributions.** UH and CL designed the chronology dataset. CL and TB compiled the metadata and prior
279 information of the chronologies. AP and TB wrote the R scripts and ran the analyses under the supervision of UH
280 and CL. AD contributed an initial R script for creating age-depth models. CL wrote the first draft of the manuscript
281 under the supervision of UH. All authors discussed the results and contributed to the final manuscript.



282 **Competing interests.** The authors declare that they have no conflict of interest.

283 **Acknowledgements.** The majority of data were obtained from the Neotoma Paleocology Database
284 (<http://www.neotomadb.org>). The work of data contributors, data stewards, and the Neotoma community is
285 gratefully acknowledged. We would like to express our gratitude to all the palynologists and geologists who, either
286 directly or indirectly, contributed pollen data and chronologies to the dataset. We thank Andrej Andreev, Mareike
287 Wieczorek, and Birgit Heim from AWI for providing information on pollen records and data uploads. We also
288 thank Cathy Jenks for language editing on a previous version of the paper. This study was undertaken as part of
289 LandCover6k, a working group of Past Global Changes (PAGES), which in turn received support from the US
290 National Science Foundation, the Swiss National Science Foundation, the Swiss Academy of Sciences, and the
291 Chinese Academy of Sciences.

292 **Financial support.** This research has been supported by the European Research Council (ERC Glacial Legacy
293 772852 to UH), the PalMod Initiative (01LP1510C to UH), and the China Scholarship Council (201908130165
294 to CL).

295 **References**

- 296 Appleby, P. G. and Oldfield, F.: The calculation of lead-210 dates assuming a constant rate of supply of
297 unsupported ^{210}Pb to the sediment, *Catena*, 5, 1–8, [https://doi.org/10.1016/S0341-8162\(78\)80002-2](https://doi.org/10.1016/S0341-8162(78)80002-2), 1978.
- 298 Bardossy, G. and Fodor, J.: Evaluation of uncertainties and risks in geology: new mathematical approaches for
299 their handling, Springer Science & Business Media, Berlin, Germany, 230 pp., 2013.
- 300 Bennett, K. D. and Fuller, J. L.: Determining the age of the mid-Holocene *Tsuga cana densis* (hemlock) decline,
301 eastern North America, *The Holocene*, 12, 421–429, <https://doi.org/10.1191/0959683602h1556rp>, 2002.
- 302 Blaauw, M.: Methods and code for ‘classical’ age-modelling of radiocarbon sequences, *Quat. Geochronol.*, 5,
303 512–518, <https://doi.org/10.1016/j.quageo.2010.01.002>, 2010.
- 304 Blaauw, M. and Christen, J. A.: Flexible paleoclimate age-depth models using an autoregressive gamma process,
305 *Bayesian Anal.*, 6, 457–474, <https://doi.org/10.1214/11-BA618>, 2011.



- 306 Blaauw, M. and Heegaard, E.: Estimation of age-depth relationships, in: Tracking Environmental Change Using
307 Lake Sediments, Volume 5: Data Handling and Numerical Techniques, edited by: Birks, H. J. B., Lotter, A. F.,
308 Juggins, S., and Smol, J. P., Springer, Dordrecht, Netherlands, 379–413, [https://doi.org/10.1007/978-94-007-](https://doi.org/10.1007/978-94-007-2745-8_12)
309 2745-8_12, 2012.
- 310 Blaauw, M., Christen, J. A., Mauquoy, D., van der Plicht, J., and Bennett, K. D.: Testing the timing of radiocarbon-
311 dated events between proxy archives, *The Holocene*, 17, 283–288, <https://doi.org/10.1177/0959683607075857>,
312 2007.
- 313 Blaauw, M., Christen, J. A., Bennett, K. D., and Reimer, P. J.: Double the dates and go for Bayes — Impacts of
314 model choice, dating density and quality on chronologies, *Quat. Sci. Rev.*, 188, 58–66,
315 <https://doi.org/10.1016/j.quascirev.2018.03.032>, 2018.
- 316 Blois, J. L., Williams, J. W. J., Grimm, E. C., Jackson, S. T., and Graham, R. W.: A methodological framework
317 for assessing and reducing temporal uncertainty in paleovegetation mapping from late-Quaternary pollen
318 records, *Quat. Sci. Rev.*, 30, 1926–1939, <https://doi.org/10.1016/j.quascirev.2011.04.017>, 2011.
- 319 Brewer, S., Giesecke, T., Davis, B. A. S., Finsinger, W., Wolters, S., Binney, H., Beaulieu, J.-L. de, Fyfe, R., Gil-
320 Romera, G., Köhl, N., Kuneš, P., Leydet, M., and Bradshaw, R. H.: Late-glacial and Holocene European pollen
321 data, *J. Maps*, 13, 921–928, <https://doi.org/10.1080/17445647.2016.1197613>, 2017.
- 322 Brown, K. J. and Hebda, R. J.: Coastal rainforest connections disclosed through a Late Quaternary vegetation,
323 climate, and fire history investigation from the Mountain Hemlock Zone on southern Vancouver Island, British
324 Columbia, Canada, *Rev. Palaeobot. Palynol.*, 123, 247–269, [https://doi.org/10.1016/S0034-6667\(02\)00195-1](https://doi.org/10.1016/S0034-6667(02)00195-1),
325 2003.
- 326 Cao, X., Ni, J., Herzsuh, U., Wang, Y., and Zhao, Y.: A late Quaternary pollen dataset from eastern continental
327 Asia for vegetation and climate reconstructions: Set up and evaluation, *Rev. Palaeobot. Palynol.*, 194, 21–37,
328 <https://doi.org/10.1016/j.revpalbo.2013.02.003>, 2013.
- 329 Cao, X., Tian, F., Andreev, A., Anderson, P. M., Lozhkin, A. V., Bezrukova, E., Ni, J., Rudaya, N., Stobbe, A.,
330 Wiczorek, M., and Herzsuh, U.: A taxonomically harmonized and temporally standardized fossil pollen
331 dataset from Siberia covering the last 40 kyr, *Earth Syst. Sci. Data*, 12, 119–135, [https://doi.org/10.5194/essd-](https://doi.org/10.5194/essd-12-119-2020)
332 12-119-2020, 2020.



- 333 Clark, P. U., Dyke, A. S., Shakun, J. D., Carlson, A. E., Clark, J., Wohlfarth, B., Mitrovica, J. X., Hostetler, S.
334 W., and McCabe, A. M.: The Last Glacial Maximum, *Science*, 325, 710–714,
335 <https://doi.org/10.1126/science.1172873>, 2009.
- 336 Clark, P. U., Shakun, J. D., Baker, P. A., Bartlein, P. J., Brewer, S., Brook, E., Carlson, A. E., Cheng, H., Kaufman,
337 D. S., Liu, Z., Marchitto, T. M., Mix, A. C., Morrill, C., Otto-Bliesner, B. L., Pahnke, K., Russell, J. M.,
338 Whitlock, C., Adkins, J. F., Blois, J. L., Clark, J., Colman, S. M., Curry, W. B., Flower, B. P., He, F., Johnson,
339 T. C., Lynch-Stieglitz, J., Markgraf, V., McManus, J., Mitrovica, J. X., Moreno, P. I., and Williams, J. W.:
340 Global climate evolution during the last deglaciation, *PNAS*, 109, E1134–E1142,
341 <https://doi.org/10.1073/pnas.1116619109>, 2012.
- 342 Cuney, M.: Nuclear geology, in: *Encyclopedia of Geology (Second Edition)*, edited by: Alderton, D. and Elias, S.
343 A., Academic Press, Cambridge, Massachusetts, United States, 723–744, <https://doi.org/10.1016/B978-0-08-102908-4.00024-2>, 2021.
- 345 Davydova, N. and Servant-Vildary, S.: Late Pleistocene and Holocene history of the lakes in the Kola Peninsula,
346 Karelia and the North-Western part of the East European plain, *Quat. Sci. Rev.*, 15, 997–1012,
347 [https://doi.org/10.1016/S0277-3791\(96\)00029-7](https://doi.org/10.1016/S0277-3791(96)00029-7), 1996.
- 348 Fiałkiewicz-koziół, B., Wachniew, P., Woszczyk, M., and Sensuła, B.: High-resolution age-depth model of a peat
349 bog in Poland as an important basis for paleoenvironmental studies, *Radiocarbon*, 109–125,
350 <https://doi.org/10.2458/56.16467>, 2014.
- 351 Flantua, S. G. A., Blaauw, M., and Hooghiemstra, H.: Geochronological database and classification system for
352 age uncertainties in Neotropical pollen records, *Clim. Past*, 12, 387–414, [https://doi.org/10.5194/cp-12-387-](https://doi.org/10.5194/cp-12-387-2016)
353 2016, 2016.
- 354 Fyfe, R. M., de Beaulieu, J.-L., Binney, H., Bradshaw, R. H. W., Brewer, S., Le Flao, A., Finsinger, W., Gaillard,
355 M.-J., Giesecke, T., Gil-Romera, G., Grimm, E. C., Huntley, B., Kunes, P., Kühl, N., Leydet, M., Lotter, A. F.,
356 Tarasov, P. E., and Tonkov, S.: The European Pollen Database: past efforts and current activities, *Veg. Hist.*
357 *Archaeobot.*, 18, 417–424, <https://doi.org/10.1007/s00334-009-0215-9>, 2009.
- 358 Gaillard, M.-J., Sugita, S., Mazier, F., Trondman, A.-K., Broström, A., Hickler, T., Kaplan, J. O., Kjellström, E.,
359 Kokfelt, U., Kuneš, P., Lemmen, C., Miller, P., Olofsson, J., Poska, A., Rundgren, M., Smith, B., Strandberg,



- 360 G., Fyfe, R. M., Nielsen, A. B., Alenius, T., Balakauskas, L., Barnekow, L., Birks, H. J. B., Bjune, A. E.,
361 Björkman, L., Giesecke, T., Hjelle, K. L., Kalnina, L., Kangur, M., van der Knaap, W. O., Koff, T., Lagerås,
362 P., Latałowa, M., Leydet, M., Lechterbeck, J., Lindbladh, M., Odgaard, B. V., Peglar, S. M., Segerström, U.,
363 von Stedingk, H., and Seppä, H.: Holocene land-cover reconstructions for studies on land cover-climate
364 feedbacks, *Clim. Past*, 6, 483–499, <https://doi.org/10.5194/cp-6-483-2010>, 2010.
- 365 Gajewski, K.: The Global Pollen Database in biogeographical and palaeoclimatic studies, *Prog. Phys. Geog.*, 32,
366 379–402, <https://doi.org/10.1177/0309133308096029>, 2008.
- 367 Giesecke, T., Bennett, K. D., Birks, H. J. B., Bjune, A. E., Bozilova, E., Feurdean, A., Finsinger, W., Froyd, C.,
368 Pokorný, P., Rösch, M., Seppä, H., Tonkov, S., Valsecchi, V., and Wolters, S.: The pace of Holocene vegetation
369 change – testing for synchronous developments, *Quat. Sci. Rev.*, 30, 2805–2814,
370 <https://doi.org/10.1016/j.quascirev.2011.06.014>, 2011.
- 371 Giesecke, T., Davis, B., Brewer, S., Finsinger, W., Wolters, S., Blaauw, M., de Beaulieu, J.-L., Binney, H., Fyfe,
372 R. M., Gaillard, M.-J., Gil-Romera, G., van der Knaap, W. O., Kuneš, P., Kühl, N., van Leeuwen, J. F. N.,
373 Leydet, M., Lotter, A. F., Ortu, E., Semmler, M., and Bradshaw, R. H. W.: Towards mapping the late
374 Quaternary vegetation change of Europe, *Veg. Hist. Archaeobot.*, 23, 75–86, [https://doi.org/10.1007/s00334-](https://doi.org/10.1007/s00334-012-0390-y)
375 012-0390-y, 2014.
- 376 Goring, S., Williams, J. W., Blois, J. L., Jackson, S. T., Paciorek, C. J., Booth, R. K., Marlon, J. R., Blaauw, M.,
377 and Christen, J. A.: Deposition times in the northeastern United States during the Holocene: establishing valid
378 priors for Bayesian age models, *Quat. Sci. Rev.*, 48, 54–60, <https://doi.org/10.1016/j.quascirev.2012.05.019>,
379 2012.
- 380 Grigg, L. D. and Whitlock, C.: Patterns and causes of millennial-scale climate change in the Pacific Northwest
381 during Marine Isotope Stages 2 and 3, *Quat. Sci. Rev.*, 21, 2067–2083, [https://doi.org/10.1016/S0277-](https://doi.org/10.1016/S0277-3791(02)00017-3)
382 3791(02)00017-3, 2002.
- 383 Hajdas, I.: Radiocarbon: calibration to absolute time scale, Elsevier, Amsterdam, Netherlands, 14, 37–43,
384 <https://doi.org/10.1016/B978-0-08-095975-7.01204-3>, 2014.



- 385 Hajdas, I. and Michczyński, A.: Age-depth model of lake Soppensee (Switzerland) based on the high-resolution
386 ^{14}C chronology compared with varve chronology, *Radiocarbon*, 52, 1027–1040,
387 <https://doi.org/10.1017/S0033822200046117>, 2010.
- 388 Heaton, T. J., Köhler, P., Butzin, M., Bard, E., Reimer, R. W., Austin, W. E. N., Ramsey, C. B., Grootes, P. M.,
389 Hughen, K. A., Kromer, B., Reimer, P. J., Adkins, J., Burke, A., Cook, M. S., Olsen, J., and Skinner, L. C.:
390 Marine20—the marine radiocarbon age calibration curve (0–55,000 cal BP), *Radiocarbon*, 62, 779–820,
391 <https://doi.org/10.1017/RDC.2020.68>, 2020.
- 392 Herzsuh, U., Cao, X., Laepple, T., Dallmeyer, A., Telford, R. J., Ni, J., Chen, F., Kong, Z., Liu, G., Liu, K.-B.,
393 Liu, X., Stebich, M., Tang, L., Tian, F., Wang, Y., Wischnewski, J., Xu, Q., Yan, S., Yang, Z., Yu, G., Zhang,
394 Y., Zhao, Y., and Zheng, Z.: Position and orientation of the westerly jet determined Holocene rainfall patterns
395 in China, *Nat. Commun.*, 10, 2376, <https://doi.org/10.1038/s41467-019-09866-8>, 2019.
- 396 Herzsuh, U., Boehmer, T., Li, C., Cao, X., Heim, B., and Wiczorek, M.: Global taxonomically harmonized
397 pollen data collection with revised chronologies, *PANGAEA*,
398 <https://doi.pangaea.de/10.1594/PANGAEA.929773>, 2021.
- 399 Hogg, A. G., Heaton, T. J., Hua, Q., Palmer, J. G., Turney, C. S., Southon, J., Bayliss, A., Blackwell, P. G.,
400 Boswijk, G., Ramsey, C. B., Pearson, C., Petchey, F., Reimer, P., Reimer, R., and Wacker, L.: SHCal20
401 Southern Hemisphere calibration, 0–55,000 years cal BP, *Radiocarbon*, 62, 759–778,
402 <https://doi.org/10.1017/RDC.2020.59>, 2020.
- 403 Hua, Q., Barbetti, M., and Rakowski, A. Z.: Atmospheric radiocarbon for the period 1950–2010, *Radiocarbon*,
404 55, 2059–2072, https://doi.org/10.2458/azu_js_rc.v55i2.16177, 2013.
- 405 Jennerjahn, T. C., Ittekkot, V., Arz, H. W., Behling, H., Pätzold, J., and Wefer, G.: Asynchronous terrestrial and
406 marine signals of climate change during Heinrich events, *Science*, 306, 2236–2239,
407 <https://doi.org/10.1126/science.1102490>, 2004.
- 408 Lane, C. S., Blockley, S. P. E., Mangerud, J., Smith, V. C., Lohne, Ø. S., Tomlinson, E. L., Matthews, I. P., and
409 Lotter, A. F.: Was the 12.1ka Icelandic Vedde Ash one of a kind?, *Quat. Sci. Rev.*, 33, 87–99,
410 <https://doi.org/10.1016/j.quascirev.2011.11.011>, 2012.



- 411 Li, C., Postl, A., Boehmer, T., Dolman, A. M., and Herzschuh, U.: Harmonized chronologies of a global late
412 Quaternary pollen dataset (LegacyAge 1.0), PANGAEA, <https://doi.pangaea.de/10.1594/PANGAEA.933132>,
413 2021.
- 414 Lowe, D. J.: Tephrochronology and its application: A review, *Quat. Geochronol.*, 6, 107–153,
415 <https://doi.org/10.1016/j.quageo.2010.08.003>, 2011.
- 416 Mottl, O., Flantua, S. G. A., Bhatta, K. P., Felde, V. A., Giesecke, T., Goring, S., Grimm, E. C., Haberle, S.,
417 Hooghiemstra, H., Ivory, S., Kuneš, P., Wolters, S., Seddon, A. W. R., and Williams, J. W.: Global acceleration
418 in rates of vegetation change over the past 18,000 years, *Science*, 372, 860–864,
419 <https://doi.org/10.1126/science.abg1685>, 2021.
- 420 Niemann, H. and Behling, H.: Late Quaternary vegetation, climate and fire dynamics inferred from the El Tiro
421 record in the southeastern Ecuadorian Andes, *J. Quat. Sci.*, 23, 203–212, <https://doi.org/10.1002/jqs.1134>, 2008.
- 422 Ojala, A. E. K., Francus, P., Zolitschka, B., Besonen, M., and Lamoureux, S. F.: Characteristics of sedimentary
423 varve chronologies – A review, *Quat. Sci. Rev.*, 43, 45–60, <https://doi.org/10.1016/j.quascirev.2012.04.006>,
424 2012.
- 425 Philippsen, B.: The freshwater reservoir effect in radiocarbon dating, *Herit. Sci.*, 1, 24,
426 <https://doi.org/10.1186/2050-7445-1-24>, 2013.
- 427 Philippsen, B. and Heinemeier, J.: Freshwater reservoir effect variability in northern Germany, *Radiocarbon*, 55,
428 1085–1101, <https://doi.org/10.1017/S0033822200048001>, 2013.
- 429 R Core Team: R: A language and environment for statistical computing, R Foundation for Statistical Computing,
430 Vienna, Austria, 2021.
- 431 Ramisch, A., Brauser, A., Dorn, M., Blanchet, C., Brademann, B., Köppl, M., Mingram, J., Neugebauer, I.,
432 Nowaczyk, N., Ott, F., Pinkerneil, S., Plessen, B., Schwab, M. J., Tjallingii, R., and Brauer, A.: VARDA
433 (VARved sediments DAtabase) – providing and connecting proxy data from annually laminated lake sediments,
434 *Earth Syst. Sci. Data*, 12, 2311–2332, <https://doi.org/10.5194/essd-12-2311-2020>, 2020.
- 435 Rasmussen, S. O., Bigler, M., Blockley, S. P., Blunier, T., Buchardt, S. L., Clausen, H. B., Cvijanovic, I., Dahl-
436 Jensen, D., Johnsen, S. J., Fischer, H., Gkinis, V., Guillevic, M., Hoek, W. Z., Lowe, J. J., Pedro, J. B., Popp,



- 437 T., Seierstad, I. K., Steffensen, J. P., Svensson, A. M., Vallelonga, P., Vinther, B. M., Walker, M. J. C.,
438 Wheatley, J. J., and Winstrup, M.: A stratigraphic framework for abrupt climatic changes during the Last
439 Glacial period based on three synchronized Greenland ice-core records: refining and extending the INTIMATE
440 event stratigraphy, *Quat. Sci. Rev.*, 106, 14–28, <https://doi.org/10.1016/j.quascirev.2014.09.007>, 2014.
- 441 Reimer, P. J., Austin, W. E. N., Bard, E., Bayliss, A., Blackwell, P. G., Ramsey, C. B., Butzin, M., Cheng, H.,
442 Edwards, R. L., Friedrich, M., Grootes, P. M., Guilderson, T. P., Hajdas, I., Heaton, T. J., Hogg, A. G., Hughen,
443 K. A., Kromer, B., Manning, S. W., Muscheler, R., Palmer, J. G., Pearson, C., van der Plicht, J., Reimer, R. W.,
444 Richards, D. A., Scott, E. M., Southon, J. R., Turney, C. S. M., Wacker, L., Adolphi, F., Büntgen, U., Capano,
445 M., Fahrni, S. M., Fogtmann-Schulz, A., Friedrich, R., Köhler, P., Kudsk, S., Miyake, F., Olsen, J., Reinig, F.,
446 Sakamoto, M., Sookdeo, A., and Talamo, S.: The IntCal20 Northern Hemisphere radiocarbon age calibration
447 curve (0–55 cal kBP), *Radiocarbon*, 62, 725–757, <https://doi.org/10.1017/RDC.2020.41>, 2020.
- 448 Roberts, N.: *The Holocene: An Environmental History* (third edition), John Wiley & Sons, Chichester, UK, 415
449 pp., 2013.
- 450 Sánchez Goñi, M. F., Desprat, S., Daniiau, A.-L., Bassinot, F. C., Polanco-Martínez, J. M., Harrison, S. P., Allen,
451 J. R. M., Anderson, R. S., Behling, H., Bonnefille, R., Burjachs, F., Carrión, J. S., Cheddadi, R., Clark, J. S.,
452 Combourieu-Nebout, N., Mustaphi, C. J. C., Debussk, G. H., Dupont, L. M., Finch, J. M., Fletcher, W. J.,
453 Giardini, M., González, C., Gosling, W. D., Grigg, L. D., Grimm, E. C., Hayashi, R., Helmens, K., Heusser, L.
454 E., Hill, T., Hope, G., Huntley, B., Igarashi, Y., Irino, T., Jacobs, B., Jiménez-Moreno, G., Kawai, S., Kershaw,
455 A. P., Kumon, F., Lawson, I. T., Ledru, M.-P., Lézine, A.-M., Liew, P. M., Magri, D., Marchant, R., Margari,
456 V., Mayle, F. E., McKenzie, G. M., Moss, P., Müller, S., Müller, U. C., Naughton, F., Newnham, R. M., Oba,
457 T., Pérez-Obiol, R., Pini, R., Ravazzi, C., Roucoux, K. H., Rucina, S. M., Scott, L., Takahara, H., Tzedakis, P.
458 C., Urrego, D. H., van Geel, B., Valencia, B. G., Vandergoes, M. J., Vincens, A., Whitlock, C. L., Willard, D.
459 A., and Yamamoto, M.: The ACER pollen and charcoal database: a global resource to document vegetation and
460 fire response to abrupt climate changes during the last glacial period, *Earth Syst. Sci. Data*, 9, 679–695,
461 <https://doi.org/10.5194/essd-9-679-2017>, 2017.
- 462 Trachsel, M. and Telford, R. J.: All age-depth models are wrong, but are getting better, *The Holocene*, 27, 860–
463 869, <https://doi.org/10.1177/0959683616675939>, 2017.



- 464 Trondman, A.-K., Gaillard, M.-J., Mazier, F., Sugita, S., Fyfe, R. M., Nielsen, A. B., Twiddle, C., Barratt, P.,
465 Birks, H. J. B., Bjune, A. E., Björkman, L., Broström, A., Caseldine, C., David, R., Dodson, J., Dörfler, W.,
466 Fischer, E., van Geel, B., Giesecke, T., Hultberg, T., Kalnina, L., Kangur, M., van der Knaap, W. O., Koff, T.,
467 Kuneš, P., Lagerås, P., Latałowa, M., Lechterbeck, J., Leroyer, C., Leydet, M., Lindbladh, M., Marquer, L.,
468 Mitchell, F. J. G., Odgaard, B. V., Peglar, S. M., Persson, T., Poska, A., Rösch, M., Seppä, H., Veski, S., and
469 Wick, L.: Pollen-based quantitative reconstructions of Holocene regional vegetation cover (plant-functional
470 types and land-cover types) in Europe suitable for climate modelling, *Global Change Biol.*, 21, 676–697,
471 <https://doi.org/10.1111/gcb.12737>, 2015.
- 472 Wang, J., Zhu, L., Wang, Y., Peng, P., Ma, Q., Haberzettl, T., Kasper, T., Matsunaka, T., and Nakamura, T.:
473 Variability of the ¹⁴C reservoir effects in Lake Tangra Yumco, Central Tibet (China), determined from recent
474 sedimentation rates and dating of plant fossils, *Quat. Int.*, 430, 3–11,
475 <https://doi.org/10.1016/j.quaint.2015.10.084>, 2017.
- 476 Williams, J. W., Grimm, E. C., Blois, J. L., Charles, D. F., Davis, E. B., Goring, S. J., Graham, R. W., Smith, A.
477 J., Anderson, M., Arroyo-Cabrales, J., Ashworth, A. C., Betancourt, J. L., Bills, B. W., Booth, R. K., Buckland,
478 P. I., Curry, B. B., Giesecke, T., Jackson, S. T., Latorre, C., Nichols, J., Purdum, T., Roth, R. E., Stryker, M.,
479 and Takahara, H.: The Neotoma Paleocology Database, a multiproxy, international, community-curated data
480 resource, *Quat. Res.*, 89, 156–177, <https://doi.org/10.1017/qua.2017.105>, 2018.
- 481 Zolitschka, B., Francus, P., Ojala, A. E. K., and Schimmelmann, A.: Varves in lake sediments – a review, *Quat.*
482 *Sci. Rev.*, 117, 1–41, <https://doi.org/10.1016/j.quascirev.2015.03.019>, 2015.